Supplementary Information for "The Penultimate deglaciation: protocol for PMIP4 transient numerical simulations between 140 and 127 ka, version 1.0"

L. Menviel[1,2,*], E. Capron[3,4,*], A. Govin[5], A. Dutton[6], L. Tarasov[7], A. Abe-Ouchi[8], R.N. Drysdale[9,10], P.L. Gibbard[11], L. Gregoire[12], F. He[13], R.F. Ivanovic[12], M. Kageyama[5], K. Kawamura[14,15,16], A. Landais[5], B.L. Otto-Bliesner[17], I. Oyabu[14], P.C. Tzedakis[18], E. Wolff[19], and X. Zhang[20,21]

[1]Climate Change Research Center, PANGEA, the University of New South Wales, Sydney, Australia
[2]Physics of Ice, Climate and Earth, Niels Bohr Institute, University of Copenhagen, Tagensvej 8, DK-2100 Copenhagen Denmark
[3]British Antarctic Survey, High Cross, Madingley Road, Cambridge, CB3 0ET, UK
[4]Laboratoire des Sciences du Climat et de l'Environnement (LSCE), Institut Pierre Simon Laplace (IPSL), CEA-CNRS-UVSQ, Université Paris-Saclay, Gif-Sur-Yvette, 91190, France
[5]Department of Geological Sciences, University of Florida, PO Box 112120, Gainesville, FL 32611, USA
[6]Department of Physics and Physical Oceanography, Memorial University of Newfoundland, St John's, Canada
[7]Atmosphere and Ocean Research Institute, The University of Tokyo, Tokyo, Japan
[8]School of Geography, The University of Melbourne, Melbourne, Australia
[9]Laboratoire EDYTEM UMR CNRS 5204, Université Savoie Mont Blanc, 73376 Le Bourget du Lac, France
[10]Scott Polar Research Institute, University of Cambridge, Cambridge, CB2 1ER, UK
[11]School of Earth and Environment, University of Leeds, Leeds, LS2 9JT, UK
[12]Center for Climatic Research, Nelson Institute for Environmental Studies, University of Wisconsin-Madison, Madison, WI 53706, USA
[13]National Institute of Polar Research, Research Organizations of Information and Systems,10-3 Midori-cho, Tachikawa, Tokyo 190-8518, Japan
[14]Department of Polar Science, Graduate University for Advanced Studies (SOKENDAI), 10-3 Midori-cho, Tachikawa, Tokyo 190-8518, Japan
[15]Institute of Biogeosciences, Japan Agency for Marine-Earth Science and Technology, 2-15 Natsushima-cho, Yokosuka 237-0061, Japan
[16]Climate and Global Dynamics Laboratory, National Center for Atmospheric Research (NCAR), Boulder, CO 80305, USA
[17]Environmental Change Research Centre, Department of Geography, University College London, London, UK
[18]Department of Earth Sciences, University of Cambridge, Cambridge, CB2 3EQ, UK
[19]Alfred Wegener Institute, Helmholtz Centre for Polar and Marine Research, D-27570 Bremerhaven, Germany
[20]Key Laboratory of Western China's Environmental Systems (Ministry of Education), College of Earth and Environmental Sciences, Lanzhou University, Lanzhou, 730000, China
[*]Both authors contributed equally to this work

Correspondence: L. Menviel (l.menviel@unsw.edu.au) and E. Capron (capron@nbi.ku.dk)

List of Supplementary Tables

3. Table S3= Tahiti corals sea-level data (Thomas et al., 2009), and recalculated ages (Hibbert et al., 2016) using new decay constants (Cheng et al., 2013)

4. Table S4= Huon peninsula corals sea-level data (Esat et al., 1999; Stein et al., 1993) and recalculated ages (Hibbert et al., 2016) using new decay constants (Cheng et al., 2013)

5. Table S5= List of the new tie points (this study) to construct the revised chronology of the Red Sea RSL record (Grant et al., 2012)

1 Corchia Cave chronology and Mg/Ca

The Corchia cave age model of Drysdale et al. (2009) was revised by updating the decay constants (Cheng et al., 2013) and rerunning the age model algorithm (Drysdale et al., 2005). This shifts the time evolution by no more than 0.5 ka across the PDG.

The Corchia Cave Mg time series is from a subaqueous speleothem (CD3) collected from the same gallery as the stalagmite (CC5) from which the Corchia δ^{18}O series has been produced. Magnesium concentrations in speleothems usually fluctuate according to changes in cave hydrology (i.e. rainfall), with lower concentrations (or lower Mg/Ca) registering periods of high recharge and high Mg concentrations (or higher Mg/Ca) corresponding to periods of low recharge (Fairchild and Baker, 2012; Drysdale et al., 2006). However, low-resolution (1 mm) δ^{18}O and Mg analysis of CD3 spanning the last four glacial-interglacial cycles shows that changes in Mg concentration follow orbital-scale temperature patterns, with higher Mg values occurring during interglacials and lower values during glacials (Figure S1). We attribute this pattern, a highly unusual phenomenon for speleothems, to the very deep location of the cave (400 m below the ground surface) and the subaqueous environment of speleothem growth, both of which would promote exceptionally slow growth rates (Drysdale et al., 2012), which in turn seems conducive to calcite precipitation at or near thermodynamic equilibrium. This has recently been shown by CD3 oxygen isotope ratios, whose water-calcite fractionation falls on the same trajectory as that for Devils Hole vein calcite (Coplen, 2007), a similarly slow-depositing speleothem. For this current study, we carried out high-resolution measurements of δ^{18}O and Mg across the PDG section of CD3, and anchored the CD3 chronology to CC5 by synchronising their δ^{18}O profiles. This enabled the Mg series of CD3 to be placed on the U-Th chronology of the 2018 Corchia Cave stalagmite stack (CCSS18, Tzedakis et al. (2018)).

2 Chronologies of marine sediment cores from the North Atlantic and the Mediterranean Sea during the Penultimate Deglaciation

The chronology of all sites during the PDG has been revised here. We use as a reference for the PDG the radiometrically-dated time scale from Corchia Cave (Italy) speleothems (Tzedakis et al., 2018). This time scale has been transferred to the western Mediterranean ODP 976 site, by aligning its SST record to the Corchia Mg record. Using the same approach, we transferred this time scale to sites MD01-2444 and MD95-2042 from the Portuguese margin, for which benthic stable isotopes

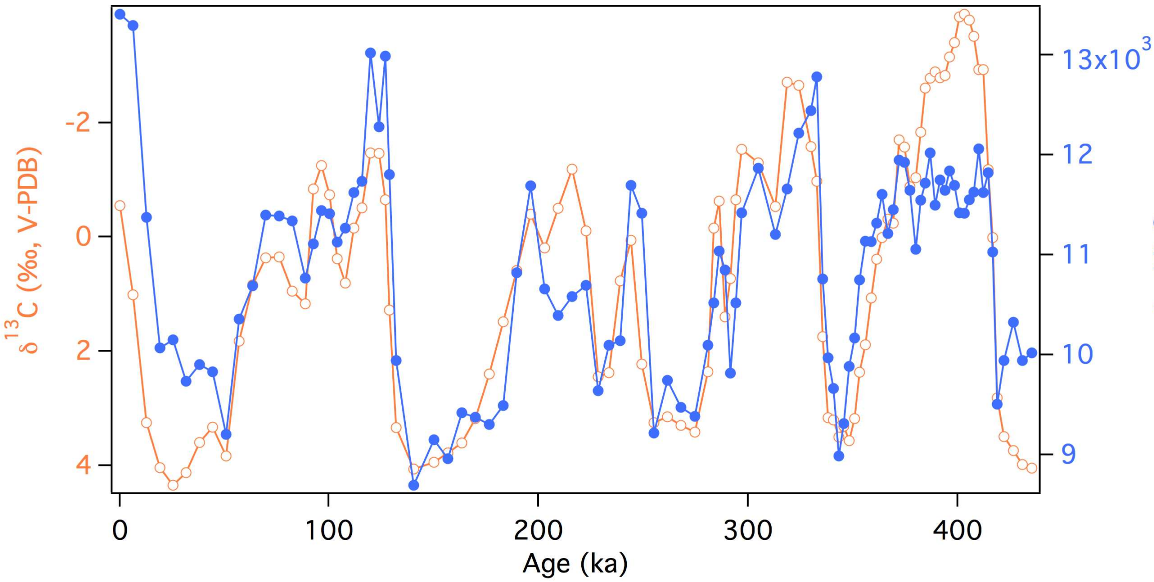

Figure S1. Low-resolution reconnaissance Mg concentrations and δ^{13}C from subaqueous speleothem CD3, cored from the same chamber in Corchia Cave from where stalagmite CC5 was collected. The Mg shows strong coherence with δ^{13}C (R=0.76, statistically significant at $p<0.05$), which is a proxy for temperature-driven changes in biogenic soil CO_2 (Drysdale et al., 2007). High values of Mg are associated with interglacials (Marine Isotope Stages (MIS) 1, 5, 7, 9 and 11), whilst low values occur during glacials (MIS 2-4, 6, 8, 10 and 12). The positive association between Mg values and warmth implies that Mg is acting as a classic palaeothermometer in this speleothem.

are available. The chronologies of other marine sites were then progressively revised during the PDG, by aligning both their benthic δ^{18}O and SST records to those of cores MD95-2042 and ODP976, respectively (see Table S1). Aligning the Iberian margin SST reconstructions onto the Corchia Mg record leads to a start of the PDG main SST increase $\sim$3 ka younger than when the SST alignment is based on the Corchia δ^{18}O record (Drysdale et al., 2009). The new PDG chronologies agree within 2 ka (not shown) with ages defined independently via the SST alignment to ice core records on AICC2012 time scale (e.g. Govin et al., 2015), supporting the chronological strategy adopted here.

Core	Latitude	Longitude	Water-depth	Alignment strategy for the PDG (140-127 ka)
ODP 976	36.20°N	4.31°W	1108 m	Alignment of ODP976 alkenone SST to U-series dated Corchia Mg
MD95-2042	37.80°N	10.17°W	3146 m	Alignment of MD95-2042 alkenone SST to U-series dated Corchia Mg
MD95-2010	66.70°N	4.57°E	1226 m	Alignment of MD95-2010 benthic $\delta^{18}O$ to MD95-2042 benthic $\delta^{18}O$ on Corchia time scale
ODP984	61.43°N	24.08°W	1649 m	Alignment of ODP984 *N. pachyderma* left percentages to ODP976 SST on Corchia time scale on Corchia time scale (agreement checked with MD95-2042 benthic $\delta^{18}O$)
ODP983	60.40°N	23.64°W	1984 m	Alignment of ODP983 *N. pachyderma* left percentages to ODP976 SST on Corchia time scale on Corchia time scale (agreement checked with MD95-2042 benthic $\delta^{18}O$)
ODP980	55.80°N	14.11°W	2180 m	Alignment of ODP980 benthic $\delta^{18}O$ to MD95-2042 benthic $\delta^{18}O$ on Corchia time scale
U1308	49.88°N	24.24°W	3883 m	Alignment of U1308 benthic $\delta^{18}O$ to MD95-2042 benthic $\delta^{18}O$ on Corchia time scale
CH69-K09	41.76°N	47.35°W	4100 m	Alignment of CH69-K09 benthic $\delta^{18}O$ and $\delta^{13}C$ to MD95-2042 benthic $\delta^{18}O$ and $\delta^{13}C$ on Corchia time scale
SU90-03	40.51°N	32.05°W	2475 m	Alignment of SU90-03 SST to ODP976 SST on Corchia time scale (agreement checked with MD95-2042 benthic $\delta^{18}O$)
MD01-2444	37.56°N	10.14°W	2637 m	Alignment of MD01-2444 alkenone SST to U-series dated Corchia Mg
ODP 1063	33.69°N	57.62°W	4584 m	Alignment of ODP1063 *N. pachyderma* left percentages to ODP976 SST on Corchia time scale (agreement checked with MD95-2042 benthic $\delta^{18}O$)

Table S1. Alignment strategies used to define the chronologies of North Atlantic and Mediterranean Sea cores for the period 140-127 ka.

References

Cheng, H., Edwards, R. L., Shen, C.-C., Polyak, V. J., Asmerom, Y., Woodhead, J., Hellstrom, J., Wang, Y., Kong, X., Spötl, C., Wang, X., and Alexander, E. C.: Improvements in 230Th dating, 230Th and 234U half-life values, and U-Th isotopic measurements by multi-collector inductively coupled plasma mass spectrometry, Earth and Planetary Science Letters, 371-372, 82–91, https://doi.org/https://doi.org/10.1016/j.epsl.2013.04.006, http://www.sciencedirect.com/science/article/pii/S0012821X13001878, 2013.

Chutcharavan, P., Dutton, A., and Ellwood, M.: Seawater 234U/238U recorded by modern and fossil corals, Geochimica et Cosmochimica Acta, 224, 1–17, https://doi.org/https://doi.org/10.1016/j.gca.2017.12.017, http://www.sciencedirect.com/science/article/pii/S0016703717307937, 2018.

Coplen, T. B.: Calibration of the calcite-water oxygen-isotope geothermometer at Devils Hole, Nevada, a natural laboratory, Geochimica et Cosmochimica Acta, 71, 3948 – 3957, https://doi.org/https://doi.org/10.1016/j.gca.2007.05.028, http://www.sciencedirect.com/science/article/pii/S0016703707003043, 2007.

Drysdale, R., Zanchetta, G., Hellstrom, J., Fallick, A., and Zhao, J.-X.: Stalagmite evidence for the onset of the Last Interglacial in southern Europe at 129 ± 1 ka, Geophysical Research Letters, 32, https://doi.org/10.1029/2005GL024658, https://agupubs.onlinelibrary.wiley.com/doi/abs/10.1029/2005GL024658, 2005.

Drysdale, R., Zanchetta, G., Hellstrom, J., Maas, R., Fallick, A., Pickett, M., Cartwright, I., and Piccini, L.: Late Holocene drought responsible for the collapse of Old World civilizations is recorded in an Italian cave flowstone, Geology, 34, 101, https://doi.org/10.1130/G22103.1, http://dx.doi.org/10.1130/G22103.1, 2006.

Drysdale, R., Zanchetta, G., Hellstrom, J., Fallick, A., McDonald, J., and Cartwright, I.: Stalagmite evidence for the precise timing of North Atlantic cold events during the early last glacial, Geology, 35, 77–80, 2007.

Drysdale, R., Hellstrom, J., Zanchetta, G., Fallick, A., Sanchez-Goni, M., Couchoud, I., McDonald, J., Maas, R., Lohmann, G., and I.Isola: Evidence for Obliquity Forcing of Glacial Termination II, Science, 325, 1527–1531, 2009.

Drysdale, R. N., Paul, B. T., Hellstrom, J. C., Couchoud, I., Greig, A., Bajo, P., Zanchetta, G., Isola, I., Spötl, C., Baneschi, I., Regattieri, E., and Woodhead, J. D.: Precise microsampling of poorly laminated speleothems for U-series dating, Quaternary Geochronology, 14, 38 – 47, https://doi.org/https://doi.org/10.1016/j.quageo.2012.06.009, http://www.sciencedirect.com/science/article/pii/S187110141200146X, 2012.

Esat, T. M., McCulloch, M. T., Chappell, J., Pillans, B., and Omura, A.: Rapid Fluctuations in Sea Level Recorded at Huon Peninsula During the Penultimate Deglaciation, Science, 283, 197–201, https://doi.org/10.1126/science.283.5399.197, http://science.sciencemag.org/content/283/5399/197, 1999.

Fairchild, I. and Baker, A.: Speleothem Science: From process to past environments, Wiley-Blackwell, 2012.

Govin, A., Capron, E., Tzedakis, P., Verheyden, S., Ghaleb, B., Hillaire-Marcel, C., St-Onge, G., Stoner, J., Bassinot, F., Bazin, L., Blunier, T., Combourieu-Nebout, N., Ouahabi, A. E., Genty, D., Gersonde, R., Jimenez-Amat, P., Landais, A., Martrat, B., Masson-Delmotte, V., Parrenin, F., Seidenkrantz, M.-S., Veres, D., Waelbroeck, C., and Zahn, R.: Sequence of events from the onset to the demise of the Last Interglacial: Evaluating strengths and limitations of chronologies used in climatic archives, Quaternary Science Reviews, 129, 1–36, 2015.

Grant, K., Rohling, E., Bar-Matthews, M., Ayalon, A., Medina-Elizalde, M., Ramsey, C. B., Satow, C., and Roberts, A.: Rapid coupling between ice volume and polar temperature over the past 150,000 years, Nature, 491, 744–747, https://doi.org/doi:10.1038/nature11593, 2012.

Hibbert, F. D., Rohling, E. J., Dutton, A., Williams, F. H., Chutcharavan, P. M., Zhao, C., and Tamisiea, M. E.: Coral indicators of past sea-level change: A global repository of U-series dated benchmarks, Quaternary Science Reviews, 145, 1 – 56, https://doi.org/https://doi.org/10.1016/j.quascirev.2016.04.019, http://www.sciencedirect.com/science/article/pii/S0277379116301305, 2016.

Stein, M., Wasserburg, G., Aharon, P., Chen, J., Zhu, Z., Bloom, A., and Chappell, J.: TIMS U-series dating and stable isotopes of the last interglacial event in Papua New Guinea, Geochimica et Cosmochimica Acta, 57, 2541 – 2554, https://doi.org/10.1016/0016-7037(93)90416-T, 1993.

Thomas, A. L., Henderson, G. M., Deschamps, P., Yokoyama, Y., Mason, A. J., Bard, E., Hamelin, B., Durand, N., and Camoin, G.: Penultimate Deglacial Sea-Level Timing from Uranium/Thorium Dating of Tahitian Corals, Science, 324, 1186–1189, https://doi.org/10.1126/science.1168754, http://science.sciencemag.org/content/324/5931/1186, 2009.

Tzedakis, P., Drysdale, R., Margari, V., Skinner, L., Menviel, L., Rhodes, R. H., Taschetto, A. S., Hodell, D. A., Crowhurst, S. J., Hellstrom, J. C., Fallick, A. E., Grimalt, J. O., McManus, J. F., Martrat, B., Mokeddem, Z., Parrenin, F., Regattieri, E., Roe, K., and Zanchetta, G.: Enhanced climate instability in the North Atlantic and southern Europe during the Last Interglacial, Nature Communications, 9, 4235, 2018.

Table S2

Tie-points			*Over an interval of ± 500 years around the tie-point age*		*Arbitrarily fixed to 400 years*	*Fixed to 500 years*				
ODP976 depth (mcd)	**Corchia age (ka)**	**Comment**	**Resolution of aligned ODP record (ka)**	**Resolution of target Corchia record (ka)**	**Matching error (ka)**	**Matching error CC Mg onto CC 18O**	**Abs age uncert -2σ (kyr)**	**Abs age uncert +2σ (kyr)**	**Final -2σ age error (ka)**	**Final +2σ age error (ka)**
39.66	127.85	Aligning SST to Corchia Mg	0.07016541	0.07	0.40	0.50	-0.64	0.68	-0.95	-0.94
40.26	129.35	Aligning SST to Corchia Mg	0.05	0.08	0.40	0.50	-0.48	0.62	-0.84	-0.90
40.63	130.31	Aligning SST to Corchia Mg	0.07	0.08	0.40	0.50	-0.79	1.16	-1.05	-1.33
41.02	132.17	Aligning SST to Corchia Mg	0.06	0.37	0.40	0.50	-1.41	1.39	-1.61	-1.57
41.82	133.74	Aligning G. bulloides d18O to Corchia d18O stack	0.07	0.15	0.40	0.50	-1.34	1.35	-1.52	-1.51
42.23	135.79	Aligning SST to Corchia Mg	0.09	0.63	0.40	0.50	-1.90	2.00	-2.12	-2.19
42.60	137.35	Aligning SST to Corchia Mg	0.08	0.32	0.40	0.50	-1.91	1.59	-2.06	-1.74
44.19	143.01	Aligning SST to Corchia Mg	0.09	0.14	0.40	0.50	-1.04	1.09	-1.26	-1.27

Table S3

TAHITI

Data from Thomas et al., (2009), and re-calculated ages from Hibbert et al., (2016)

Sample ID	Elevation (m)	Corr Elev (m)	Age (ka)	2σ uncert (ka)	$\delta^{234}U$ init (‰)	2σ uncert (‰)	Screened Ages (ka)	Avg Age per coral (ka)	2σ uncert per coral (ka)	Corr Elev per coral (m)
310-M0005D-20R-2W-0,21	-117.52	-84.47	132.2	0.9	148.8	1.2	132.2	136.9	0.4	-83.3
310-M0005D-20R-2W-0,21	-117.52	-83.09	137.7	0.4	148.6	1.1	137.7			
310-M0005D-20R-2W-14,21	-117.66	-84.31	133.4	1.0	157.5	1.2				
310-M0005D-20R-2W-14,21	-117.66	-84.26	133.6	0.4	148.2	1.1	133.6	133.6	0.4	-84.3
310-M0009D-25R-1W-64,70	-145.82	-108.83	148.0	0.9	144.6	1.2	148.0	148.0	0.9	-108.8
310-M0009D-25R-1W-95,102	-146.13	-109.76	145.5	0.9	164.4	1.2				
310-M0009D-25R-2W-41,49	-146.95	-108.82	152.5	0.7	143.0	0.8	152.5	152.7	0.4	-108.8
310-M0009D-25R-2W-41,49	-146.95	-108.76	152.8	0.5	144.2	1.2	152.8			
310-M0009D-25R-2W-52,55	-147.06	-108.78	153.1	0.7	144.8	0.8	153.1	153.2	0.4	-108.8
310-M0009D-25R-2W-52,55	-147.06	-108.75	153.2	0.5	144.3	1.2	153.2			
310-M0019A-27R-1W-62,83	-115.24	-81.98	133.0	0.4	149.9	1.1	133.0	133.0	0.3	-82.0
310-M0019A-27R-1W-62,83	-115.24	-81.98	133.1	0.9	151.1	1.4	133.1			
310-M0019A-27R-1W-62,83	-115.24	-81.76	133.9	0.4	149.5	1.1	133.9			
310-M0019A-29R-1W-0,4	-117.61	-83.50	136.5	0.9	150.5	1.4	136.5	137.5	0.4	-83.2
310-M0019A-29R-1W-0,4	-117.61	-83.19	137.7	0.4	150.5	1.1	137.7			
310-M0019A-29R-1W-16,24	-117.77	-84.05	134.9	0.9	170.1	1.4				-117.8
310-M0019A-29R-1W-16,24	-117.77	-83.83	135.8	0.4	170.7	1.1				
310-M0019A-32R-1W-0,4	-119.61	-85.92	134.8	0.9	155.8	1.5				-119.6
310-M0019A-32R-1W-0,4	-119.61	-85.40	136.8	0.4	155.2	1.1				

Table S3 legend (columns from left to right)

Col 1: Sample ID for all individual measurements

Col 2: Elevation relative to mean sea level (MSL)

Col 3: Back-calculated elevation corrected for subsidence and using the Age in col. 6

Col 4: Age in thousands of years ago (ka), as re-calculated in Hibbert et al. (2016) using the decay constants of Cheng et al. (2013) for ^{230}Th and ^{234}U

Col 5: 2-sigma age uncertainty, as reported in Hibbert et al. (2016)

Col 6: Initial $\delta^{234}U$ value, back-calculated using the age in col. 4, as reported in Hibbert et al. (2016)

Col 7: 2-sigma uncertainty in initial $\delta^{234}U$ value, as reported in Hibbert et al. (2016)

Col 8: Ages passing screening criteria (within 5 ‰ of modern seawater value = 145 ‰, Chutcharavan et al., (2018)

Col 9: Inverse-variance weighted means per coral of subsamples passing the screening criteria

Col 10: 2-sigma uncertainty of inverse variance-weighted means in col. 9

Col 11: Back-calculated elevation corrected for subsidence using the inverse-variance weighted means in col.9

Table S4

HUON PENINSULA *(original data from Esat et al. (1999) and Stein et al. (1993) and re-calculated ages from Hibbert et al. (2016)).*

Sample ID	Elevation (m)	Corr Elev (m)	Age (ka)	2σ uncert (ka)	$\delta^{234}U$ init (‰)	2σ uncert (‰)	Screened Ages (ka)	Avg Age per coral (ka)	2σ uncert per coral (ka)	Corr Elev per coral (m)
AC-U10	142.7	-66.4	134.1	0.6	154.7	2.7	134.1	134.1	0.6	-66.4
AC-U11-bottom	142.7	-56.9	127.9	0.3	157.8	1.3				
AC-U11a-top	142.7	-53.7	125.9	0.4	154.1	1.3	125.9	125.9	0.4	-53.7
AC-U11b-top	142.7	-53.8	126	1.1	142.7	4.0	126.0			
AC-U13a	142.7	-60.7	130.4	0.4	154.6	1.3	130.4	130.4	0.4	-60.7
AC-U13b	142.7	-58.9	129.2	0.6	159.8	2.7				
AC-U14	142.7	-60.4	130.2	0.6	153.1	2.7	130.2	130.2	0.6	-60.4
AC-U19	142.7	-60.6	130.3	0.6	156.0	2.7	130.3	130.3	0.6	-60.6
AC-U21	142.7	-61.8	131.1	0.6	147.6	2.7	131.1	**131.1**	0.6	-61.8
AC-U24	142.7	-65.2	133.3	0.7	150.0	2.7	133.3	**133.3**	0.7	-65.2
HP-23	197	-56.6	137.1	1.9	154.6	1.6	137.1	137.1	1.9	-56.6
Kanz-1p	139.9	-83.6	143.2	0.9	163.3	2.7				
Kanz-U4	139.9	-36.5	138.0	0.5	162.4	1.4				
Kwam-U4	170.8	-84.5	138.0	0.5	162.4	1.4				
Kwam-U9p	170.8	-70.5	130.4	0.8	160.4	2.7				
Kwan-U5	142.7	-63.2	132.0	0.6	139.3	2.7	132.0	**132.0**	0.6	-63.2
Kwan-U9p	142.7	-57.8	128.5	0.6	145.1	2.7	128.5	**128.5**	0.6	-57.8
HP-16-a	215	-68.0	153.0	2.5	193.8	9.5				
HP-16-b	215	-47.5	141.9	1.4	190.8	5.4				
HP-16-c	215	-39.0	137.3	2.4	183.9	10.7				
HP-17	212	-60.8	147.5	2.5	174.2	8.2				
HP-22	217	-36.1	136.8	1.8	150.0	6.8	136.8	**136.8**	1.8	-36.1
HP-23-a	217	-34.4	135.9	1.3	143.8	5.4	135.9	**134.5**	1.3	-34.4
HP-23-b	217	-29.1	133.0	1.2	146.9	5.4	133.0			
KIL-4	224	-30.3	137.5	2.4	164.9	9.4				
SIAL-M-1	185	-45.8	124.8	1.3	180.4	6.5				
SIAL-M-3	203	-46.9	135.1	1.9	160.9	8.1	135.1	135.1	1.9	-46.9

Table S4 legend:
Col 1: Sample ID for corals with ages between 125 and 150 ka
col 2: Elevation relative to mean sea level (MSL)
col 3: Back-calculated elevation corrected for uplift and using the Age in col. 4
col 4: Age in thousands of years ago (ka), as re-calculated in Hibbert et al. (2016) using the decay constants of Cheng et al. (2013) for ^{230}Th and ^{234}U
col 5: 2-sigma age uncertainty, as reported in Hibbert et al. (2016)
col 6: Initial $\delta^{234}U$ value, back-calculated using the age in col. 4, as reported in Hibbert et al. (2016)
col 7: 2-sigma uncertainty in initial $\delta^{234}U$ value, as reported in Hibbert et al. (2016)
col. 8: Ages passing screening criteria (within 10 ‰ of modern seawater value = 145 ‰, Chutcharavan et al. (2018)). For comparison, $\delta^{234}U$ data within 5 ‰ of modern seawater are denoted in bold font)
col 9: Inverse-variance weighted means per coral of subsamples passing the screening criteria
col. 10: 2-sigma uncertainty of inverse variance-weighted means in col.9
col. 11: Back-calculated elevation corrected for uplift using the inverse-variance weighted means in col.9

Table S5

Cols. 1-3: Red Sea SL from Grant et al (2012).
Col. 4: Modified age model with tie points (in blue bold)

Age (ka BP)	RSL data (m)	±2s (ky)	Proposed Age Model (ka)	Tie point comment
0.0689059	0.74	0.070489009	0.0689059	
0.221817	7.24	0.0740021324	0.221817	
0.323748	-2.28	0.0763439911	0.323748	
0.476659	-0.1	0.0798571123	0.476659	
0.578597	-6.19	0.0821991318	0.578597	
0.731501	3.72	0.0857120921	0.731501	
0.807953	8.11	0.0874685723	0.807953	
0.83344	-2.17	0.0880541346	0.83344	
0.986344	-0.81	0.0915670949	0.986344	
1.07916	-11.2	0.093699537	1.07916	
1.08828	1.31	0.0939090685	1.08828	
1.17077	-2.51	0.0958042713	1.17077	
1.2157	1.48	0.0968365354	1.2157	
1.24119	-2.32	0.0974221667	1.24119	
1.26238	8.16	0.0979090057	1.26238	
1.34312	2.025	0.0997640024	1.34312	
1.35399	-0.61	0.10001374	1.35399	
1.41958	-2.89	0.1015206663	1.41958	
1.44559	1.49	0.1021182445	1.44559	
1.53721	1.84	0.1042232086	1.53721	
1.59797	-4.81	0.105619166	1.59797	
1.62881	-0.27	0.1063277132	1.62881	
1.6999	-2.47	0.1079610017	1.6999	
1.72042	-1.32	0.1084324475	1.72042	
1.81203	5.69	0.1105371818	1.81203	
1.85281	4.02	0.1114740999	1.85281	
1.90364	6.04	0.1126419161	1.90364	
1.95475	4.91	0.1138161654	1.95475	
1.99524	3.58	0.1147464207	1.99524	
2.08686	10.25	0.1168513848	2.08686	
2.10765	-2.67	0.1173290338	2.10765	
2.17846	-1.61	0.1189558894	2.17846	
2.20959	-4.4	0.1196710993	2.20959	
2.27007	-2.83	0.1210606237	2.27007	
2.36168	-4.32	0.123165358	2.36168	
2.36249	3.08	0.1231839677	2.36249	
2.43895	6.96	0.1249406317	2.43895	
2.45329	-3.16	0.1252700923	2.45329	
2.46443	0.63	0.1255260331	2.46443	
2.54489	-1.62	0.1273745969	2.54489	
2.61734	0.09	0.1290391313	2.61734	
2.6365	-1.99	0.1294793312	2.6365	
2.71927	-5.46	0.131380967	2.71927	
2.72811	0.76	0.1315840655	2.72811	
2.81972	-1	0.1336887998	2.81972	
2.87219	-6.36	0.134894295	2.87219	
2.91133	-0.65	0.1357935342	2.91133	
2.97412	-2.05	0.1372361307	2.97412	
3.00293	-1.35	0.1378980387	3.00293	

3.09455	-3.49	0.1400030028	3.09455
3.12703	-1.34	0.1407492289	3.12703
3.18615	-6.76	0.1421075074	3.18615
3.22897	-3.85	0.1430912943	3.22897
3.27776	8.12	0.1442122417	3.27776
3.36937	1.8	0.146316976	3.36937
3.38187	-6.25	0.1466041628	3.38187
3.45832	2.7	0.148360597	3.45832
3.46098	1.8	0.1484217103	3.46098
3.48381	-12.52	0.1489462282	3.48381
3.55258	13.03	0.1505262149	3.55258
3.63671	-7.22	0.1524590966	3.63671
3.69414	-0.31	0.1537785475	3.69414
3.73865	1.32	0.1548011621	3.73865
3.83568	0.74	0.1570304206	3.83568
3.89155	-8.76	0.1583140305	3.89155
3.97723	-0.67	0.1602825235	3.97723
3.99349	-9.47	0.160656096	3.99349
4.11878	-5.62	0.1635346263	4.11878
4.1464	-9.49	0.1641691942	4.1464
4.24834	-6.81	0.1665112596	4.24834
4.26033	-3.2	0.1667867292	4.26033
4.40124	-13.47	0.1700241281	4.40124
4.40188	-3.93	0.170038832	4.40188
4.47769	-9.02	0.1717805623	4.47769
4.50318	-3.39	0.1723661935	4.50318
4.54343	-3.2	0.1732909349	4.54343
4.65608	-10.71	0.175879062	4.65608
4.68498	-4.37	0.1765430378	4.68498
4.75802	-6.99	0.1782211274	4.75802
4.82653	-11.67	0.1797951406	4.82653
4.91092	-9.41	0.1817339959	4.91092
4.96807	-21.11	0.1830470137	4.96807
5.01286	-13.5	0.1840760613	5.01286
5.16577	-13.43	0.1875891595	5.16577
5.25117	-10.19	0.1895512194	5.25117
5.2677	-3.39	0.1899309952	5.2677
5.39272	-6.8	0.1928033223	5.39272
5.42062	-12.32	0.1934443231	5.42062
5.49707	-14.43	0.1952007574	5.49707
5.52255	-2.84	0.1957861588	5.52255
5.53427	1.4	0.1960554252	5.53427
5.67546	-10.09	0.199299257	5.67546
5.67582	-15.62	0.199307528	5.67582
5.7774	0.24	0.2016413225	5.7774
5.81737	-3.96	0.2025596309	5.81737
5.9303	-11.16	0.2051541909	5.9303
5.95892	-12.5	0.2058117337	5.95892
6.03224	2.47	0.2074962564	6.03224
6.10047	0.34	0.2090638366	6.10047
6.18514	-11.31	0.2110091248	6.18514
6.24202	-3.97	0.2123159394	6.24202
6.28708	0.56	0.2133511903	6.28708
6.38356	-2.44	0.2155678126	6.38356
6.43998	-7.74	0.2168640587	6.43998
6.51644	-0.31	0.2186207227	6.51644
6.52511	-13.28	0.2188199154	6.52511

6.57135	-10.43	0.2198822767	6.57135
6.66666	-9.88	0.2220720183	6.66666
6.7684	-4.38	0.2244094887	6.7684
6.80821	-5.26	0.2253241211	6.80821
6.9478	-3.97	0.2285311931	6.9478
6.94976	1.02	0.228576224	6.94976
7.04982	-0.74	0.2308750966	7.04982
7.14988	-12.12	0.2331739691	7.14988
7.21689	-7.54	0.2347135199	7.21689
7.24994	-24.08	0.2354728417	7.24994
7.35	-28.07	0.2377717143	7.35
7.37853	-10.94	0.2388581119	7.37853
7.41167	-25.18	0.2401200544	7.41167
7.47334	-17.35	0.2424683945	7.47334
7.535	-10.24	0.2448163539	7.535
7.54437	-8.83	0.2451731553	7.54437
7.59667	-28.08	0.247164694	7.59667
7.65493	-5.54	0.2493831843	7.65493
7.65834	-29.14	0.2495130341	7.65834
7.72	-4.01	0.2518609935	7.72
7.78167	-5.29	0.2542093336	7.78167
7.82078	-11.13	0.2556986085	7.82078
7.84334	-26.97	0.2565576737	7.84334
7.9037	-14.02	0.2588561302	7.9037
7.90501	-23.39	0.2589060138	7.90501
7.93134	-10.87	0.2599086374	7.93134
7.96668	-17.37	0.261254354	7.96668
8.02835	-25.96	0.2636026941	8.02835
8.09001	-23.8	0.2659506534	8.09001
8.09719	-15.97	0.2662240616	8.09719
8.15168	-12.15	0.2682989936	8.15168
8.20775	1.86	0.2704340906	8.20775
8.21335	-26.28	0.2706473337	8.21335
8.27501	-15.99	0.272995293	8.27501
8.33668	-15.69	0.2753436332	8.33668
8.37359	-16.98	0.276749134	8.37359
8.39835	-7.71	0.2776919733	8.39835
8.46002	-21.69	0.2800403134	8.46002
8.48415	-9.91	0.2809591629	8.48415
8.52169	-28.42	0.2823886536	8.52169
8.58335	-21.21	0.2847366129	8.58335
8.64502	-14.66	0.287084953	8.64502
8.65	-39.69	0.2872745871	8.65
8.85124	-26.29	0.3310961083	8.85124
9.07016	-13.35	0.3787675822	9.07016
9.63121	-26.94	0.5009404329	9.63121
9.92557	-26.23	0.5650395333	9.92557
10.05	-54.36	0.5921351002	10.05
10.5092	-26.42	0.7690625623	10.5092
10.85	-41.09	0.9003710968	10.85
10.9097	-26.9	0.9233732081	10.9097
11.65	-63.26	1.2086070935	11.65
12.45	-77.02	1.5168430901	12.45
13.1536	-72.82	1.991901138	13.1536
13.8571	-75.37	2.4668916676	13.8571
17.45	-87.07	3.6703447263	17.45
23.085	-115.74	5.009605185	23.085

26.0553	-99.13	3.3425333753	26.0553
26.9694	-104.88	2.8294975402	26.9694
27.2725	-97.83	2.6593835903	27.2725
27.5748	-102	2.4897186379	27.5748
27.8762	-105.64	2.3205588077	27.8762
28.1767	-103.92	2.1519040999	28.1767
28.4763	-105.31	1.9837545143	28.4763
28.7749	-99.82	1.8161661756	28.7749
29.0726	-106.44	1.6490829592	29.0726
29.3693	-108.08	1.4825609897	29.3693
29.6651	-104.99	1.3165441425	29.6651
29.9598	-106.95	1.1511446669	29.9598
30.1953	-92.91	1.0189710107	30.1953
30.2535	-103.79	0.9863064383	30.2535
30.4135	-92.31	0.8965069266	30.4135
30.468	-90.51	0.8659189679	30.468
30.5461	-103.28	0.8220855813	30.5461
30.7097	-96.7	0.7302655806	30.7097
30.7406	-91.97	0.7129230499	30.7406
30.8325	-97.55	0.6613444554	30.8325
30.9549	-101.36	0.592647829	30.9549
30.9587	-88.96	0.5905150906	30.9587
31.0768	-94.78	0.524231826	31.0768
31.1727	-79.43	0.5253095517	31.1727
31.2419	-80.33	0.5260872224	31.2419
31.2681	-87.76	0.5263816584	31.2681
31.3632	-83.69	0.5274503937	31.3632
31.4578	-90.95	0.5285135099	31.4578
31.5521	-85.19	0.5295732548	31.5521
31.6459	-73.19	0.5306273807	31.6459
31.6571	-90.8	0.5307532464	31.6571
31.7394	-83.88	0.5316781351	31.7394
31.8324	-92.1	0.5327232706	31.8324
31.925	-77.4	0.5337639108	31.925
32.0172	-83.14	0.5348000558	32.0172
32.109	-85.01	0.5358317057	32.109
32.2004	-86.29	0.5368588603	32.2004
32.2799	-81.97	0.5377522825	32.2799
32.2913	-81.64	0.5378803959	32.2913
32.3817	-78.86	0.5388963125	32.3817
32.4718	-87.19	0.5399088577	32.4718
32.5614	-72.59	0.5409157839	32.5614
32.6505	-94.63	0.5419170911	32.6505
32.7392	-80.85	0.5429139031	32.7392
32.7935	-87.52	0.5435241273	32.7935
32.8275	-90.13	0.5439062199	32.8275
33.0027	-84.46	0.5458751202	33.0027
33.0896	-91.11	0.5468517037	33.0896
33.262	-77.4	0.5487891376	33.262
33.3475	-81.25	0.549749988	33.3475
33.4326	-95.38	0.5507063431	33.4326
33.5172	-82.03	0.5516570792	33.5172
33.5641	-85.94	0.5521841421	33.5641
33.6014	-82.03	0.5526033201	33.6014
33.6851	-79.43	0.553543942	33.6851
33.7684	-88.16	0.5544800687	33.7684
33.8511	-85.01	0.5554094526	33.8511

33.9335	-75.33	0.5563354651	33.9335
34.0777	-87.7	0.5579559869	34.0777
34.0967	-88.16	0.5581695092	34.0967
34.1777	-86.84	0.5590797885	34.1777
34.2061	-88.28	0.5593989481	34.2061
34.3382	-90.48	0.56088349	34.3382
34.4178	-85.74	0.561778036	34.4178
34.4969	-89.29	0.562666963	34.4969
34.5756	-90.95	0.5635513949	34.5756
34.6538	-94.63	0.5644302077	34.6538
34.7316	-89.44	0.5653045253	34.7316
34.8089	-88.84	0.5661732239	34.8089
34.9389	-76.48	0.577025801	34.9389
35.0634	-72.99	0.5874192306	35.0634
35.3166	-85.01	0.6085567116	35.3166
35.5683	-78.04	0.6295689704	35.5683
35.8186	-77	0.6504643554	35.8186
36.0674	-74.06	0.6712345184	36.0674
36.3148	-70.15	0.6918878074	36.3148
36.5609	-70.9	0.7124325707	36.5609
36.64	-82.19	0.7190359465	36.64
36.8055	-68.39	0.7328521119	36.8055
37.0487	-64.61	0.7531547792	37.0487
37.2905	-72.99	0.7733405726	37.2905
37.531	-79.05	0.7934178403	37.531
37.7702	-86.29	0.8133865821	37.7702
38.008	-90.48	0.8332384501	38.008
38.2445	-93.84	0.8529817923	38.2445
38.4797	-85.92	0.8726166087	38.4797
38.7136	-82.23	0.8921428994	38.7136
38.9463	-79.63	0.9115690124	38.9463
39.1777	-87.37	0.9308865996	39.1777
39.1916	-80.26	0.9320469906	39.1916
39.4079	-84.83	0.9501040092	39.4079
39.6369	-85.19	0.9692212412	39.6369
39.8646	-81.25	0.9882299474	39.8646
40.0912	-85.55	1.0071468241	40.0912
40.3167	-80.25	1.0259718713	40.3167
40.541	-79.24	1.0446967409	40.541
40.7643	-85.74	1.0633381291	40.7643
40.865	-90.95	1.0717447023	40.865
40.9864	-77.4	1.0818793397	40.9864
41.2075	-76.6	1.1003370689	41.2075
41.4275	-68.64	1.1187029686	41.4275
41.6466	-88.55	1.1369937351	41.6466
41.8646	-82.03	1.155192672	41.8646
42.0817	-88.99	1.1733164758	42.0817
42.2979	-84.46	1.1913651463	42.2979
42.5131	-83.88	1.2093303355	42.5131
42.7275	-84.08	1.2272287396	42.7275
42.941	-74.29	1.2450520104	42.941
43.1537	-68.89	1.2628084962	43.1537
43.3656	-86.84	1.2804981969	43.3656
43.3752	-74.49	1.281299618	43.3752
43.5767	-88.84	1.2981211125	43.5767
43.7871	-86.48	1.3156855911	43.7871
43.9967	-78.66	1.3331832847	43.9967

44.1316	-78.81	1.3444449204	44.1316
44.2057	-77.2	1.3506308894	44.2057
44.4141	-80.04	1.3680284053	44.4141
44.6218	-80.25	1.3853674842	44.6218
44.829	-78.04	1.4026648225	44.829
45.0357	-75.33	1.4199204201	45.0357
45.2418	-68.64	1.4371259289	45.2418
45.2661	-79.85	1.439154526	45.2661
45.4474	-72.59	1.454289697	45.4474
45.6526	-80.65	1.4714200725	45.6526
45.8575	-72.12	1.4885254037	45.8575
46.0226	-83.16	1.5023081766	46.0226
46.0619	-78.25	1.5055889941	46.0619
46.266	-70.9	1.5226275402	46.266
46.4699	-65.72	1.5396493899	46.4699
46.6735	-74.06	1.5566461953	46.6735
46.8768	-84.83	1.5736179563	46.8768
47.08	-85.55	1.5905813691	47.08
47.1571	-83.19	1.5970177821	47.1571
47.2831	-89.29	1.6075364338	47.2831
47.4861	-90.95	1.6244831503	47.4861
47.689	-79.84	1.6414215188	47.689
47.892	-90.13	1.6583682353	47.892
47.9135	-85.67	1.6601630846	47.9135
48.0949	-92.43	1.6753066037	48.0949
48.298	-101.49	1.6922616684	48.298
48.4051	-86.48	1.7047587718	48.4051
48.568	-86.29	1.723766971	48.568
48.6162	-83.36	1.7293912509	48.6162
48.7311	-82.03	1.7427985075	48.7311
48.8944	-77.61	1.7618533812	48.8944
48.9371	-85.9	1.7668358865	48.9371
49.0579	-78.04	1.7809315922	49.0579
49.2218	-78.04	1.8000564777	49.2218
49.3859	-78.66	1.8192047005	49.3859
49.4184	-77.95	1.8229970055	49.4184
49.5505	-70.15	1.8384112665	49.5505
49.7154	-81.05	1.8576528383	49.7154
49.7392	-83.63	1.8604299724	49.7392
49.8807	-74.52	1.8769410847	49.8807
50.0466	-78.47	1.8962993428	50.0466
50.2129	-75.75	1.9157042754	50.2129
50.2205	-76.56	1.9165910914	50.2205
50.3798	-76.6	1.9351792199	50.3798
50.5414	-79.13	1.9540357269	50.5414
50.5473	-61.96	1.9547241761	50.5473
50.6216	-74.41	1.9633939686	50.6216
50.8843	-67.32	1.9940474612	50.8843
51.0226	-72.04	2.0101851773	51.0226
51.0539	-74.06	2.0138374587	51.0539
51.2242	-73.83	2.0337091365	51.2242
51.3053	-75.29	2.0431723959	51.3053
51.3954	-69.14	2.0536858321	51.3954
51.5674	-72.12	2.0737558767	51.5674
51.7293	-74.07	2.0926473896	51.7293
51.7403	-65.72	2.093930939	51.7403
51.9142	-63.59	2.1142226876	51.9142

52.0052	-80.16	2.1248411414	52.0052
52.089	-64.93	2.1346194538	52.089
52.2649	-60.34	2.155144575	52.2649
52.419	-74.39	2.1731259347	52.419
52.4419	-57.08	2.1757980511	52.4419
52.62	-40.27	2.1965798822	52.62
52.7078	-72.46	2.1952062592	52.7078
52.8301	-41.81	2.1932928867	52.8301
53.0417	-54.5	2.1899824239	53.0417
53.1927	-74.42	2.1876200425	53.1927
53.2547	-72.59	2.1866500582	53.2547
53.4692	-68.12	2.1832942251	53.4692
53.516	-68.8	2.1825620433	53.516
53.5968	-79.33	2.1812979346	53.5968
53.6854	-70.15	2.1799117956	53.6854
53.9033	-70.15	2.1765027699	53.9033
54.0009	-79.03	2.1749758267	54.0009
54.1229	-61.96	2.1730671477	54.1229
54.3241	-84.55	2.1699193919	54.3241
54.3443	-70.65	2.1696033648	54.3443
54.5675	-65.72	2.166111421	54.5675
54.7927	-66.57	2.1625881873	54.7927
54.8899	-83.53	2.1610675021	54.8899
54.8909	-75.18	2.1610518572	54.8909
55.0198	-75.54	2.1590352284	55.0198
55.0515	-84.7	2.1585392848	55.0515
55.2489	-57.66	2.1554509796	55.2489
55.4802	-71.14	2.1518323121	55.4802
55.5364	-79.35	2.1509530681	55.5364
55.5375	-70.46	2.1509358587	55.5375
55.7136	-70.65	2.1481807902	55.7136
55.9493	-83.14	2.144493285	55.9493
56.1829	-76.98	2.1408386342	56.1829
56.184	-68.06	2.1408214248	56.184
56.1872	-72.99	2.140771361	56.1872
56.4275	-92.75	2.1370118893	56.4275
56.6702	-80.65	2.1332148698	56.6702
56.8295	-71.91	2.1307226357	56.8295
56.8305	-70.17	2.1307069908	56.8305
56.9154	-75.54	2.1293787379	56.9154
57.1631	-51.74	2.1255034939	57.1631
57.4135	-62.23	2.1215860085	57.4135
57.476	-69.02	2.1206082017	57.476
57.4771	-65.32	2.1205909923	57.4771
57.6665	-66.57	2.1176278464	57.6665
57.9223	-59.52	2.1136258786	57.9223
58.0948	-62.41	2.1109271317	58.0948
58.0959	-61.71	2.1109099223	58.0959
58.181	-55.5	2.1095785405	58.181
58.4425	-60.34	2.1054873966	58.4425
58.5668	-66.37	2.1035427344	58.5668
58.5679	-67.54	2.103525525	58.5679
58.707	-66.57	2.1013493181	58.707
58.9745	-69.14	2.0971643048	58.9745
59.0389	-72.76	2.0961567726	59.0389
59.04	-70.32	2.0961395632	59.04
59.2451	-65.72	2.0929307923	59.2451

59.511	-73.62	2.0887708108	59.511
59.5121	-68.44	2.0887536014	59.5121
59.5189	-66.57	2.0886472161	59.5189
59.7959	-57.39	2.0843135761	59.7959
60.0763	-53.51	2.0799267435	60.0763
60.1011	-65.89	2.0795387497	60.1011
60.1021	-73.99	2.0795231048	60.1021
60.36	-61.96	2.0754882827	60.36
60.4551	-72.07	2.0740004518	60.4551
60.4562	-72.01	2.0739832424	60.4562
60.5731	-70.38	2.0721543525	60.5731
60.6472	-74.52	2.0709950647	60.6472
60.9272	-69.43	2.06661449	60.9272
60.9282	-76.89	2.0665988451	60.9282
60.9379	-64.13	2.0664470895	60.9379
61.2323	-78.47	2.0618412281	61.2323
61.3992	-71.72	2.0592300927	61.3992
61.4003	-93.28	2.0592128833	61.4003
61.5304	-62.77	2.0571774806	61.5304
61.8322	-62.77	2.0524558469	61.8322
61.9395	-95.39	2.0507771481	61.9395
61.9404	-100.51	2.0506822827	61.9404
62.1021	-93.84	2.0336381242	62.1021
62.2535	-93.36	2.017679648	62.2535
62.3964	-86.39	2.0026171233	62.3964
62.3972	-97.12	2.0025327984	62.3972
62.405	-81.64	2.0017106312	62.405
62.5564	-86.84	1.9857521551	62.5564
62.7078	-94	1.9697936789	62.7078
62.8593	-104.31	1.9538246621	62.8593
62.9674	-103.1	1.942430268	62.9674
62.9683	-95.3	1.9423354025	62.9683
62.9692	-101.34	1.9422405371	62.9692
63.0107	-95.67	1.9378661859	63.0107
63.1622	-97.13	1.9218971692	63.1622
63.3136	-100.45	1.905938693	63.3136
63.4242	-92.05	1.8942807837	63.4242
63.4251	-102.14	1.8941859183	63.4251
63.4651	-97.69	1.8899696762	63.4651
63.6165	-101.23	1.8740112001	63.6165
63.7679	-94.78	1.8580527239	63.7679
63.881	-95.35	1.8461312995	63.881
63.8819	-102.17	1.846036434	63.8819
63.9194	-98.84	1.8420837071	63.9194
64.0708	-100.84	1.826125231	64.0708
64.2223	-101.49	1.8101562142	64.2223
64.3379	-96.69	1.7979712746	64.3379
64.3387	-103.32	1.7978869498	64.3387
64.3737	-108.69	1.794197738	64.3737
64.5251	-100.07	1.7782392618	64.5251
64.6766	-94.48	1.7622702451	64.6766
64.7947	-91.48	1.7498217904	64.7947
64.7956	-104.3	1.749726925	64.7956
64.828	-98.12	1.7463117689	64.828
64.9795	-99.43	1.7303427521	64.9795
65.1309	-98.69	1.714384276	65.1309
65.2515	-97.59	1.7016723062	65.2515

65.2524	-94.25	1.7015774407	65.2524
65.2533	-101.4	1.7014825753	65.2533
65.2824	-101.87	1.6984152592	65.2824
65.4338	-101.36	1.682456783	65.4338
65.5852	-98.84	1.6664983068	65.5852
65.7083	-96.9	1.6535228219	65.7083
65.7367	-86.11	1.6505292901	65.7367
65.8881	-95.82	1.6345708139	65.8881
66.0396	-85.19	1.6186017971	66.0396
66.1651	-91.33	1.6053733377	66.1651
66.166	-97.2	1.6052784722	66.166
66.191	-80.85	1.602643321	66.191
66.3425	-95.82	1.5866743042	66.3425
66.4939	-94.93	1.570715828	66.4939
66.622	-88.69	1.5572133128	66.622
66.6229	-97	1.5571184474	66.6229
66.6453	-84.65	1.5547573518	66.6453
66.7968	-80.45	1.5387883351	66.7968
66.9482	-89.9	1.5228298589	66.9482
67.0788	-92.23	1.5090638286	67.0788
67.0797	-98.4	1.5089689632	67.0797
67.5356	-100.48	1.4609143444	67.5356
67.5365	-97.06	1.4608194789	67.5365
67.5374	-100.02	1.4607246135	67.5374
67.9924	-97.24	1.4127648601	67.9924
67.9933	-98.29	1.4126699947	67.9933
68.3351	-94.01	1.3766422063	68.3351
68.336	-94.02	1.3765473409	68.336
68.9061	-85.99	1.316455351	68.9061
68.907	-90.88	1.3163604856	68.907
69.081	-83.26	1.2980198327	69.081
69.4762	-77.67	1.2563633612	69.4762
69.4771	-85.63	1.2562684957	69.4771
69.9291	-78.3	1.2086249605	69.9291
69.93	-84.01	1.2085300951	69.93
70.08	-82.53	1.1927191874	70.08
70.9186	-70.44	1.2466808628	70.9186
70.9203	-78.71	1.2467902533	70.9203
71.7483	-49.5	1.3000698469	71.7483
72.0367	-60.01	1.3186276184	72.0367
72.0383	-73.04	1.3187305742	72.0383
73.1548	-54.93	1.390574374	73.1548
73.1564	-70.88	1.3906773298	73.1564
74.0493	-72.63	1.4481330655	74.0493
74.2728	-63.02	1.4625146949	74.2728
74.2745	-78.15	1.4626240854	74.2745
75.6704	-70.89	1.5524465308	75.6704
75.9499	-47.03	1.570431611	75.9499
75.9516	-69.07	1.5705410014	75.9516
76.3502	-35.09	1.5961898493	76.3502
77.068	-49.45	1.6423783666	77.068
77.0696	-59.44	1.6424813223	77.0696
78.1861	-42.2	1.7143251222	78.1861
78.1877	-60.01	1.7144280779	78.1877
79.0346	-70.22	1.7689238362	79.0346
79.3041	-41.12	1.7862654431	79.3041
79.305	-66.39	1.7862147967	79.305

79.7162	-43.82	1.7630750438	79.7162
79.717	-64.02	1.7630300248	79.717
80.2656	-53.23	1.732158263	80.2656
80.2664	-49.23	1.732113244	80.2664
80.2673	-61.47	1.7320625977	80.2673
80.815	-47.79	1.7012414822	80.815
80.8158	-54.3	1.7011964632	80.8158
81.3644	-31.23	1.6703247013	81.3644
81.3652	-49.98	1.6702796824	81.3652
81.9138	-31.94	1.6394079205	81.9138
81.9147	-53.23	1.6393572742	81.9147
82.4632	-36.58	1.6084911397	82.4632
82.4641	-49.19	1.6084404934	82.4641
83.0126	-43.59	1.5775743589	83.0126
83.0135	-32.95	1.5775237125	83.0135
83.0143	-40.98	1.5774786936	83.0143
83.5059	-42.22	1.5498145337	83.5059
83.6307	-30.65	1.5427915736	83.6307
83.6315	-43.07	1.5427465546	83.6315
84.2488	-27.45	1.5080087884	84.2488
84.2496	-32.11	1.5079637694	84.2496
84.3862	-40.93	1.5002767795	84.3862
84.7295	-45.66	1.480958012	84.7295
84.8669	-48.57	1.4732260031	84.8669
84.9356	-38.96	1.4693599986	84.9356
85.0042	-26.92	1.4654996216	85.0042
85.2396	-29.9	1.4522527883	85.2396
85.5536	-33.96	1.4345828408	85.5536
86.103	-58.24	1.4036660599	86.103
86.3777	-58.74	1.3882076695	86.3777
86.7898	-75.28	1.3650172702	86.7898
87.0645	-50.6	1.3495588798	87.0645
87.2649	-79.96	1.3382816267	87.2649
87.4766	-80.51	1.3263684805	87.4766
87.6826	-67.14	1.3147760946	87.6826
88.0574	-63.78	1.2936847049	88.0574
88.1222	-79.03	1.290038168	88.1222
88.7793	-75.85	1.3516410285	88.7793
89.0422	-63.72	1.3762877976	89.0422
89.4365	-63.65	1.4132532639	89.4365
89.6993	-46.13	1.4378906581	89.6993
89.8233	-63.26	1.4495156082	89.8233
90.0936	-59.65	1.4748561244	90.0936
90.2908	-48.83	1.493343545	90.2908
90.3565	-48.5	1.4995028935	90.3565
90.7508	-57.64	1.5364683598	90.7508
91.0136	-47.43	1.561105754	91.0136
91.1488	-52.59	1.5737806996	91.1488
91.4079	-57.27	1.5980712202	91.4079
91.6707	-49.44	1.6227086144	91.6707
92.065	-59.94	1.6596740807	92.065
92.3279	-52.18	1.6843208499	92.3279
92.7222	-59.2	1.7212863161	92.7222
92.9193	-56.46	1.7397643618	92.9193
92.985	-46.39	1.7459237103	92.985
93.3793	-58.32	1.7828891766	93.3793
93.5692	-48.66	1.8006922251	93.5692

93.6421	-48.81	1.8075265708	93.6421
94.0364	-57.8	1.8444920371	94.0364
94.2993	-48	1.8691388062	94.2993
94.6936	-57.19	1.9061042725	94.6936
94.9564	-41.88	1.9307416667	94.9564
95.3507	-54.06	1.9677071329	95.3507
95.5478	-41.56	1.9861851786	95.5478
95.6135	-33.35	1.9923445271	95.6135
95.9783	-54.42	2.0265443803	95.9783
96.0078	-55.27	2.0293099934	96.0078
96.2707	-37.97	2.0539567626	96.2707
96.665	-54.57	2.0909222288	96.665
96.9278	-35.83	2.115559623	96.9278
97.3221	-50.52	2.1525250893	97.3221
97.585	-30.98	2.1771718585	97.585
97.942	-43.09	2.2106404647	97.942
97.9792	-50.6	2.2141279498	97.9792
98.1764	-37.74	2.2326153704	98.1764
98.2421	-30.21	2.2387747189	98.2421
98.6364	-45.58	2.2757401852	98.6364
98.8992	-33.37	2.3003775794	98.8992
99.2935	-43.91	2.3373430457	99.2935
99.5564	-33.49	2.3619898148	99.5564
99.9506	-45.03	2.3989459061	99.9506
100.117	-32.29	2.4145458391	100.117
100.213	-32.81	2.4235458005	100.213
100.608	-40.33	2.4605768915	100.608
100.805	-41.41	2.4790455622	100.805
100.982	-17.85	2.4562156086	100.982
102.043	-40.02	2.31936487	102.043
102.751	-12.29	2.2280450557	102.751
103.812	-36.99	2.0911943171	103.812
104.52	-17.62	1.9998745029	104.52
105.377	-51.04	1.8893362531	105.377
105.459	-43.33	1.8796133073	105.459
105.74	-19.4	1.8462944319	105.74
106.163	-47.82	1.7961382601	106.163
106.374	-31.04	1.7711194605	106.374
106.444	-25.12	1.7628193848	106.444
106.867	-33.26	1.712663213	106.867
107.148	-12.03	1.6793443376	107.148
107.464	-38.87	1.6418754244	107.464
107.57	-31.34	1.6293067383	107.57
107.852	-1.77	1.5958692904	107.852
108.274	-36.8	1.5458316911	108.274
108.556	-36.1	1.5123942433	108.556
108.978	-56.74	1.462356644	108.978
109.189	-39.19	1.4373378443	109.189
109.26	-48.82	1.4289191961	109.26
109.548	-55.27	1.3947703132	109.548
109.682	-70.83	1.3788815968	109.682
109.982	-46.87	1.384402848	109.982
110.433	-64.75	1.3927031291	110.433
110.778	-30.24	1.399052568	110.778
111.251	-38.94	1.4077577408	111.251
111.295	-55.35	1.4085675243	111.295
111.64	-27.16	1.4149169633	111.64

112.157	-51.15	1.4244319196	112.157
112.416	-34.72	1.4291985998	112.416
112.502	-29.94	1.4307813585	112.502
112.52	-44.94	1.4311126336	112.52
113.019	-47.26	1.4402963148	113.019
113.364	-28.54	1.4466457537	113.364
113.365	-28.26	1.4466641579	113.365
113.882	-46.18	1.4561791142	113.882
114.226	-27.24	1.462510149	114.226
114.744	-48.66	1.4720435095	114.744
115.089	-18.35	1.4783929484	115.089
115.175	-36.29	1.4799757071	115.175
115.606	-43.54	1.4879079047	115.606
115.865	-34.03	1.4926745849	115.865
115.951	-19.86	1.4942573436	115.951
116.111	-44.37	1.497202011	116.111
116.468	-36.62	1.5037722999	116.468
116.813	-23.82	1.5101217389	116.813
117.33	-33.39	1.5196366952	117.33
117.675	-22.68	1.5259861341	117.675
118.192	-27.43	1.5355010904	118.192
118.433	-46.29	1.5399364956	118.433
118.537	-13.08	1.5418505293	118.537
119.054	-31.77	1.5513654857	119.054
119.313	-18.03	1.5561321659	119.313
119.399	-15.94	1.5577149246	119.399
119.917	-23.56	1.5672482851	119.917
120.262	-11.31	1.573597724	120.262
120.523	-10.83	1.5784012126	120.523
120.779	-18.66	1.5831126803	120.779
121.124	3.02	1.5894621192	121.124
121.641	-23.47	1.5989770756	121.641
121.972	-11.22	1.6050688561	121.972
121.986	-11.14	1.6053265145	121.986
122.503	-16.1	1.6148414708	122.503
122.504	-22.16	1.614859875	122.504
122.676	-3.3	1.6180253923	122.676
122.762	-9.12	1.619608151	122.762
122.848	-10.24	1.6211909097	122.848
123.02	-5.62	1.6243564271	123.02
123.193	-0.67	1.6275403487	123.193
123.365	-8.46	1.630705866	123.365
123.366	-21.59	1.6307242702	123.366
123.42	-17.14	1.6317180954	123.42
123.538	7.15	1.6338897876	123.538
123.71	-0.88	1.637055305	123.71
123.783	-0.17	1.6383988094	123.783
123.883	2.59	1.6402392265	123.883
124.055	1.46	1.6434047439	124.055
124.145	-7.93	1.6450611193	124.145
124.227	5.46	1.6465702613	124.227
124.228	-17.69	1.6465886654	124.228
124.326	1.65	1.6483922742	124.326
124.507	-11.27	1.6517234291	124.507
124.572	-1.78	1.6529197002	124.572
124.745	-2.81	1.6561036218	124.745
124.869	-8.69	1.6583857389	124.869

125.09	-12.63	1.6624530607	125.09	
125.231	-3.89	1.6650480488	125.231	
125.594	0.53	1.6717287628	125.594	
125.952	-6.95	1.6783174559	125.952	
125.956	7.06	1.6783910726	125.956	
126.318	-3.54	1.6850533824	126.318	
126.68	-4.28	1.6917156923	126.68	
127.042	3.79	1.6983780021	127.042	
127.405	8.47	1.7050587161	127.405	
127.767	7.03	1.711721026	127.767	
127.948	16.11	1.7150521809	127.948	
128.129	12.33	1.7183833358	128.129	
128.491	-0.26	1.7250456456	128.491	
128.853	-3.22	1.7317079555	128.853	
129.216	7	1.7383886695	129.216	
129.578	11.6	1.7450509793	**129.578**	* Tie point unchanged from Grant et al. (2012) age, chosen at onset of sea level highstand for the interglacial
129.94	-6.2	1.7517132891	129.87386386	
130.121	-12.49	1.755044444	130.02179578	
130.262	-3.06	1.7576394321	130.13703557	
130.302	-2.51	1.758375599	130.16972771	
130.664	-14.34	1.7650379088	130.46559157	
131.027	-14.35	1.7717186228	130.76227273	
131.091	-42.75	1.7728964897	130.81458015	
131.249	4.32	1.7758043487	130.9437141	
131.389	-16.56	1.7783809326	131.05813658	
131.407	-26.39	1.7787122077	131.07284805	
131.565	-16.34	1.7816200667	131.20198199	
131.724	-16.68	1.7845463299	131.33193325	
131.882	18.37	1.7874541888	131.46106719	
131.883	-34.91	1.787472593	131.4618845	
131.906	-20.96	1.7878958889	131.48068248	
132.04	-14.48	1.7903620478	131.59020114	
132.113	-25.29	1.7917055523	131.6498643	
132.198	-49.26	1.7932699068	131.71933509	
132.629	-36.47	1.8012021044	132.07159289	
132.672	-58.79	1.8019934838	132.10673693	
132.909	-68.54	1.8063552723	132.30043786	
132.988	-68.53	1.8078092018	132.36500483	
133.058	-41.16	1.8090974937	132.42221607	
133.463	-72.62	1.8165511829	132.75322398	
133.488	-51.6	1.8170112872	132.77365657	
133.779	-72.75	1.8223669009	133.01149188	
133.917	-55.76	1.8249066764	133.12427975	
134.132	-76.16	1.8288635732	**133.3**	* Tie point chosen using mean of ages from two Tahiti corals marking the end of MWP-2A
134.253	-75.99	1.8310904778	133.36808826	
134.346	-72.3	1.8328020657	133.42042055	
134.57	-76.75	1.8369246	133.54646824	
134.776	-76.4	1.8407158592	133.66238709	
135.044	-81.59	1.845648177	133.81319414	
135.205	-75.3	1.8486112485	133.90379091	
135.635	-73.49	1.8565250419	134.14575744	
135.835	-69.28	1.8150549085	134.25830001	

136.092	-70.67	1.8815071137	134.40291722	
136.104	-82.68	1.8846099404	134.40966978	
136.807	-73.05	2.0663838713	134.80525692	
137.027	-80.16	2.1232690275	134.92905375	
137.523	-76.01	2.2515191978	135.20815934	
138.238	-78.83	2.4363959554	135.61049904	
138.344	-83.17	2.4638042579	135.6701466	
138.954	-46.76	2.6215312819	136.01340145	
139.311	-96.63	2.7138403763	136.21428995	
139.661	-84.48	2.8043394884	136.41123945	
139.669	-50.19	2.8064080395	136.41574115	
140.385	-60.68	2.991543366	136.81864357	
140.51	-35.94	3.0238644775	136.88898267	
140.76	-95.58	3.0885067004	137.02966089	
140.885	-78.87	3.1208278119	**137.1**	* Tie point chosen using mean of ages from four corals from Tahiti and Huon Peninsula marking the beginning of MWP-2A
140.978	-90.77	3.1448747188	137.38509514	
141.26	-93.07	3.2177911463	138.24957717	
141.323	-97.56	3.2340809865	138.44270613	
141.385	-96.36	3.2501122578	138.63276956	
141.502	-94.82	3.2543440042	138.99143763	
141.589	-99.48	3.2574906874	139.25813953	
141.831	-101.16	3.2662435303	**140**	* Tie point chosen using estimated age of onset of RSL rise from linear age-depth model
142.553	-92.61	3.2923573842	140.84031934	
142.723	-96.89	3.2985060755	141.03817847	
143.275	-89.56	3.318471238	141.68063868	
143.543	-99.61	3.328164469	141.99255777	
143.997	-87.86	3.3445850918	142.52095802	
144.259	-98.17	3.3540613102	142.82589385	
144.286	-97.54	3.3550378671	142.85731854	
144.719	-88.05	3.3706989456	143.36127737	
144.975	-79.82	3.3799581514	143.65922993	
145.441	-84.26	3.3968127994	144.20159671	
145.73	-91.39	3.4072655747	144.53795722	
145.793	-84.1	3.4095442073	144.61128148	
146.164	-89.6	3.422962822	145.04307992	
146.609	-85.67	3.4390579258	145.56100528	
146.886	-85.39	3.4490766758	145.88339927	
147.102	-91.14	3.4568891307	146.13479674	
147.175	-91.24	3.4595294511	146.21975978	
147.319	-87.41	3.4647377543	146.3873581	
147.464	-83.73	3.4699822263	146.55612029	
147.608	-93.13	3.4751905296	146.72371861	
147.609	-86.1	3.4752266984	146.72488248	
147.627	-93.06	3.4758777363	146.74583227	
147.752	-82.48	3.4803988329	146.89131692	
147.897	-94.21	3.4856433049	147.06007912	
148.135	-92.09	3.4942514728	147.33708189	
148.186	-95.3	3.4960960802	147.39643963	
148.33	-84.05	3.5013043834	147.56403795	
148.475	-82.36	3.5065488554	147.73280014	
148.619	-90.03	3.5117571587	147.90039846	

148.845	-95.57	3.5199313013	148.16343471	
148.908	-90.92	3.522209934	148.23675897	
149.052	-83.72	3.5274182372	148.40435729	
149.053	-88.34	3.527454406	148.40552117	
149.197	-90.51	3.5326627092	148.57311948	
149.341	-94.75	3.5378710125	148.7407178	
149.413	-87.65	3.5404751641	148.82451696	
149.63	-90.04	3.5483237878	149.07707831	
149.775	-96.17	3.5535682598	149.24584051	
150.16	-89.69	3.5674932373	149.69393323	
150.497	-95.22	3.5796821136	150.08615985	
151.066	-95	3.6002621452	150.74840598	
151.219	-98.52	3.6057959674	150.92647919	
151.769	-100.79	3.6256887924	151.56661165	
151.921	-98.72	3.6311864458	151.74352099	
152.463	-86.21	3.6507899205	152.37434243	
152.625	-90.43	3.6566492617	152.56289054	
153.004	-87.82	3.6703572265	**153.004**	* Tie point chosen to match age from Grant et al. (2012)